



Investigating the vertical extent of the 2023 summer Canadian wildfire impacts with satellite observations

Selena Zhang¹, Susan Solomon¹, Chris D. Boone², and Ghassan Taha^{3,4}

¹Department of Earth, Atmospheric, and Planetary Sciences, Massachusetts Institute of Technology, Cambridge, MA 02139, USA

²Department of Chemistry, University of Waterloo, Waterloo, Ontario N2L 3G1, Canada

³Goddard Earth Sciences Technology and Research (GESTAR) II, Morgan State University, Baltimore, MD 21251, USA

⁴NASA Goddard Space Flight Center, Greenbelt, MD 20771, USA

Correspondence: Selena Zhang (selenaxz@mit.edu)

Received: 5 February 2024 – Discussion started: 28 February 2024

Revised: 28 August 2024 – Accepted: 9 September 2024 – Published: 21 October 2024

Abstract. Pyrocumulonimbus clouds (pyroCb) generated by intense wildfires can serve as a direct pathway for the injection of aerosols and gaseous pollutants into the lower stratosphere, resulting in significant chemical, radiative, and dynamical changes. Canada experienced an extremely severe wildfire season in 2023, with a total area burned that substantially exceeded those of previous events known to have impacted the stratosphere (such as the 2020 Australian fires). This season also had record-high pyroCb activity, which raises the question of whether the 2023 Canadian event resulted in significant stratospheric perturbations. Here, we investigate this anomalous wildfire season using retrievals from multiple satellite instruments, ACE-FTS (Atmospheric Chemistry Experiment – Fourier transform spectrometer), OMPS LP (Ozone Mapping and Profiler Suite Limb Profiler), and MLS (Microwave Limb Sounder), to determine the vertical extents of the wildfire smoke along with chemical signatures of biomass burning. These data show that smoke primarily reached the upper troposphere, and only a nominal amount managed to penetrate the tropopause. Only a few ACE-FTS occultations captured elevated abundances of biomass-burning products in the lowermost stratosphere. OMPS LP aerosol measurements also indicate that any smoke that made it past the tropopause did not last long enough or reach high enough to significantly perturb stratospheric composition. While this work focuses on Canadian wildfires given the extensive burned area, pyroCb at other longitudes (e.g., Siberia) are also captured in the compositional analysis. These results highlight that despite the formation of many pyroCb in major wildfires, those capable of penetrating the tropopause are extremely rare; this in turn means that even a massive area burned is not necessarily an indicator of stratospheric effects.

1 Introduction

In 2023, a record-breaking fire season burned over 15 Mha in Canada, over 7 times the 1983–2022 annual average burned area of 2.1 Mha (Canadian Interagency Forest Fire Centre Inc., 2024, <https://ciffc.net/statistics/>, last access: 10 January 2024). These events follow a trend of increasingly extensive and destructive wildfires, often referred to as megafires, that are projected to become more frequent under a changing climate (Di Virgilio et al., 2019; Williams et al., 2019; Pausas and Keeley, 2021). In addition to the well-studied impacts

of megafires on air quality and tropospheric composition, a number of events have also injected wildfire smoke into the stratosphere via deep convective events known as pyrocumulonimbus clouds (pyroCb) (Fromm et al., 2010, 2019, 2022).

PyroCb are towering thunderstorms triggered by intense surface fire activity that also require specific meteorological conditions for development (including very dry surface conditions and high moisture and instability in the mid-troposphere; see Peterson et al., 2017). Strong evidence has been presented to show that past wildfire events injected significant amounts of smoke above the tropopause and that

smoke-charged vortices may also self-loft (Khaykin et al., 2020; Renard et al., 2020; Lestrelin et al., 2021; Sellitto et al., 2023). Perhaps the most notable example of these effects is the 2019–2020 Australian New Year Super Outbreak (ANYSO) event that injected up to 1.1 Tg of smoke into the stratosphere (Peterson et al., 2021). ANYSO, which was part of the Australian “Black Summer” bushfire season where around 5.8 Mha burned, has been linked to stratospheric ozone depletion and numerous climate impacts (Boer et al., 2020; Kablick et al., 2020; Rieger et al., 2021; Bernath et al., 2022; Solomon et al., 2023). While the Black Summer fires raged for about 7 months, nearly all the stratospheric input occurred in just a few days: 29–31 December 2019 and 4 January 2020 (Davey and Sarre, 2020; Khaykin et al., 2020; Peterson et al., 2021). Stratospheric perturbations also occurred as a result of the 2017 Pacific Northwest Event (PNE) in British Columbia, when on 12 August 2017, pyroCbs injected an estimated 0.3 Tg of aerosols into the stratosphere (Peterson et al., 2018; Torres et al., 2020). For context compared to 2023, the 2017 Canadian wildfires burned a total of 3.5 Mha, with over 1.2 Mha burned in British Columbia (Government of British Columbia, 2024, <https://www2.gov.bc.ca/gov/content/safety/wildfire-status/about-bcws/wildfire-history/wildfire-season-summary>, last access: 10 January 2024).

Given the outsized area burned in the 2023 Canadian wildfires, significant stratospheric impacts, perhaps as in the PNE or ANYSO events, might be expected. It has been reported that at least 135 pyroCbs occurred in Canada between May and August 2023, a record-high amount, further suggesting the possibility of substantial perturbations to stratospheric composition (Smith, 2023). Recent research has investigated the tropospheric impacts of the 2023 fires, identifying record-high particulate matter emissions with implications for air quality and human health, but the vertical extent of these impacts and whether smoke entered the stratosphere have not yet been reported (Thurston et al., 2023; Wang et al., 2023).

The Atmospheric Chemistry Experiment – Fourier transform spectrometer (ACE-FTS) is a satellite instrument that detects a number of species, including multiple biomass-burning tracers with high sensitivity and precision (Sect. 2.1). Here, we use data from ACE as well as aerosol extinction data from the Ozone Mapping and Profiler Suite Limb Profiler (OMPS LP), described in Sect. 2.2, to investigate whether the 2023 Canadian wildfires perturbed stratospheric composition. Microwave Limb Sounder (MLS) carbon monoxide data are also analyzed.

2 Data and methods

2.1 ACE-FTS and MLS data

ACE-FTS aboard the Canadian ACE–SCISAT-1 platform is a solar occultation instrument that collects up to 30 daily atmospheric absorption measurements at sunrise and sunset us-

ing the Sun as a light source (Bernath, 2005, 2017). The infrared Fourier transform spectrometer measures over a wide spectral range (750 to 4400 cm^{-1}) with a high resolution of 0.02 cm^{-1} and signal-to-noise ratio ranging between 100 : 1 and 400 : 1 (Buijs et al., 2013). The ACE-FTS processing version 5.2 provides vertical volume mixing ratio (VMR) profiles for 46 molecules and 24 isotopologues, including characteristic biomass-burning indicator molecules such as carbon monoxide (CO), hydrogen cyanide (HCN), acetonitrile (CH_3CN), and ethane (C_2H_6) (Boone et al., 2023). A pair of filtered imagers also measure atmospheric extinction at two wavelengths: visible (VIS, 527.11 nm) and near-infrared (NIR, 1020.55 nm). The NIR imager is less likely to become saturated in cases of strong aerosol extinction and was thus used in this analysis for detection of aerosol loads (Vanhellemont et al., 2008; Boone et al., 2020). Temperature profiles are also collected with every occultation and were used to calculate tropopause heights (Sect. 2.3). Data from ACE are available at https://database.scisat.ca/level2/ace_v5.2/ (last access: 25 August 2024) starting from 2004 (Boone et al., 2023).

Given the limited data coverage of ACE, we also analyze carbon monoxide data from the MLS aboard the NASA Aura satellite (Waters et al., 2006) given its higher spatial coverage. The MLS instrument has seven radiometers that measure microwave thermal emissions between 118 GHz and 2.5 THz from the limb of the atmosphere to determine vertical profiles of atmospheric constituents. This instrument has a much higher spatial coverage than ACE, but the use of microwave spectroscopy provides data with a lower signal-to-noise ratio on individual soundings and a more limited vertical range. For example, the CO data product is recommended for scientific use between 215–0.001 hPa, while the HCN and CH_3CN valid ranges are even smaller at 21–0.1 and 46–1.0 hPa, respectively (Livesey et al., 2022). Since we are interested in the vertical profiles of biomass-burning products, MLS is not as useful as ACE for our analysis, given the lack of reliable data at our pressure range of interest in the lowermost stratosphere and its transition to the tropopause and upper troposphere. However, carbon monoxide data from MLS in the lower stratosphere are still useful as complementary data since strong signals from large perturbations would be clearly detected (Fig. S1 in the Supplement). Additionally, comparison of ACE and MLS profiles in our latitude range of interest supports our conclusions from ACE data despite more limited coverage (Fig. S2). Data from MLS are available at https://disc.gsfc.nasa.gov/datasets/ML2CO_NRT_005/summary (last access: 25 August 2024) starting from 2004 (EOS MLS Science Team, 2022).

2.2 OMPS LP aerosol data

OMPS LP on the Suomi NPP satellite is a limb profiler that measures scattered UV, visible, and near-IR radiation. Aerosol extinction coefficients are retrieved for six wave-

lengths (510, 600, 675, 745, 849, and 997 nm) with the V2.1 algorithm (Taha et al., 2021). OMPS LP measures along Earth's limb with three parallel vertical slits: one central slit that views along the nadir track and two side slits viewing with a cross-track separation of 250 km at the tangent point, allowing for near-global daily coverage. The 745 nm channel was used in this analysis given its high sensitivity to aerosol loading and low bias, and aerosol extinction is analyzed as an indicator of aerosol abundance. A cloud detection algorithm detects the highest cloud altitude and flags all aerosol extinction measurements below the peak cloud level, allowing for a cloud-filtered data product (Chen et al., 2016). The retrieved aerosol-to-molecular extinction ratio analyzed in this work is analogous to an aerosol mixing ratio; see Loughman et al. (2018) and Taha et al. (2022) for a detailed account of the retrieval algorithm and previous data applications. Data from OMPS are available at https://disc.gsfc.nasa.gov/datasets/OMPS_NPP_LP_L2_AER_DAILY_2/summary (last access: 25 August 2024; Taha, 2020).

2.3 Tropopause height calculation

Determination of stratospheric entry depends on the definition of tropopause height. Given the high variability of tropopause heights, using data that are specific to the time and location of the VMR and aerosol extinction measurements of interest is important. Concurrent temperature profiles are retrieved alongside VMR profiles from ACE; specifically, ACE temperature profiles are determined from 18 km upwards from data retrievals, while temperatures and pressures below 18 km are fixed to data from the Canadian Meteorological Centre weather model (Sica et al., 2008). Therefore, a temperature-based tropopause definition, the WMO lapse rate tropopause, was used in this study (WMO, 1957).

In practice, the lapse rate tropopause was calculated by first determining the lapse rate of the ACE temperature profile at every vertical level and interpolating to determine slope values between the 1 km vertical intervals. Every vertical level where the lapse rate reached -2 K km^{-1} was marked, and the lowest level at which the lapse rate passed this threshold was determined to be the tropopause altitude. For temperature profiles that exhibit a double tropopause, this method provides the lower tropopause altitude (Peevey et al., 2012; Homeyer et al., 2014).

3 Results and discussion

3.1 Chemical signatures for biomass burning

The tropopause acts as a strong barrier to troposphere-to-stratosphere transport, and the high vertical resolution of ACE is useful in determining whether smoke entered the stratosphere. Individual occultation measurements from ACE provide simultaneous constituent VMR and tempera-

ture profiles where biomass-burning product VMRs can be compared against self-consistent tropopause heights as measured on the same occultation and on broader averages. HCN is a robust wildfire tracer for the Northern Hemisphere because its primary source is biomass burning (Li et al., 2000; Roberts et al., 2020). In contrast, other tracers like CO and ethane are emitted in large amounts by both wildfires and anthropogenic sources such as transportation and industry (Xiao et al., 2004), complicating source attribution for those compounds. Additionally, wildfires are not the only source of particles in the stratosphere, especially in the recent context of the Hunga Tonga–Hunga Ha'apai and Shiveluch eruptions in the last couple of years. This is why we focus on chemical data from ACE-FTS in addition to aerosol data to be able to confidently attribute wildfires as the source.

We first investigate average monthly HCN VMR profiles. Some individual occultations do not extend into the troposphere, so monthly averages in absolute altitude capture the maximum amount of data to compare 2023 with the rest of the ACE-FTS measurement period (2004 to 2022). A tropopause-relative framework is used in Sect. 3.2 to detect individual measurements of stratospheric smoke. Chemical anomalies detected in the region from 40 to 70° N that are likely associated with wildfires also reflect other active burning regions such as Siberia (MODIS Land Rapid Response Team, 2023, https://modis.gsfc.nasa.gov/gallery/individual.php?db_date=2023-07-05, last access: 27 February 2024). Figure 1 suggests an enhancement of HCN in the upper troposphere and lowermost stratosphere (UTLS) between June and September 2023 relative to preceding years, with the monthly average tropopause heights calculated from ACE-FTS temperature profiles representing a rough delineation between the troposphere and stratosphere. On average, enhancements do not extend more than a couple kilometers above the tropopause. Similar results can be seen for single profiles (Fig. S3).

ACE–SCISAT-1 takes a very limited number of measurements over our latitude range of interest during August, as seen in Table S1; only 20 measurements were taken in August 2023 and all on the first couple of days of the month between 40 and 45° N. This may explain the unusually high tropopause altitude for this month as tropopause altitudes are higher closer to the Equator, and previous studies with ACE in August also report a higher tropopause height (Doeringer et al., 2012). Additionally, a low number of measurements are likely more susceptible to transient meteorological influences such as the Asian monsoon (Basha et al., 2020). ERA5 reanalysis data collocated at ACE measurement points and times for August yield a similarly high average tropopause height of 14.6 km (Hersbach et al., 2023).

The range given by the standard deviation of ACE data from 2004 to 2022 indicates that there were likely other wildfire years that also produced high HCN mixing ratios from June to September, but 2023 is on the upper end of this spread from about 8 to 11 km. July 2023 in particular has notice-

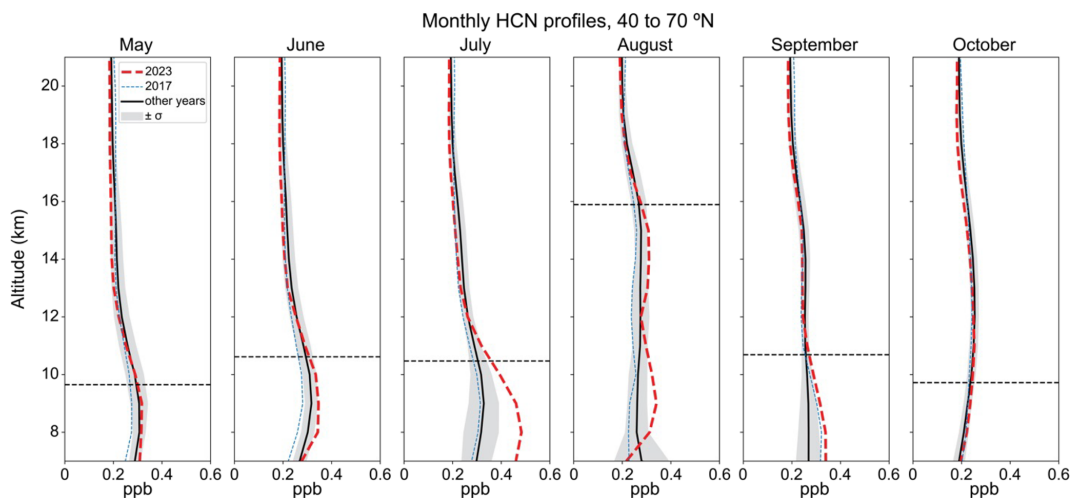


Figure 1. Monthly average HCN profiles from 40 to 70°N measured by ACE-FTS. The red curves show monthly averages in 2023, and the black curves show monthly averages from 2004–2022 with the grey-shaded area representing ± 1 standard deviation from the 2004–2022 average. The dashed blue line indicates 2017 averages, as it was an anomalous year with the PNE. The monthly average lapse rate tropopause altitudes calculated for 2023 are plotted as horizontal dashed lines for reference.

ably higher abundances compared to the range of previous years. Although this HCN enhancement is indicative of wildfire smoke reaching the upper troposphere, the occurrence of stratospheric injection is less clear given the variability of tropopause heights and the limited number of observations, particularly in August (see Table S1). This limited coverage and amount of August ACE data are supplemented by the higher coverage of OMPS as shown in the following section and MLS in the Supplement.

The average July 2023 profiles of other biomass-burning markers such as CO, CH₃OH, HCOOH, and C₂H₆ also exhibit elevated VMRs in the upper troposphere but not significantly so in the lowermost stratosphere (Fig. 2).

These data provide strong evidence of the vertical transport of wildfire smoke to the upper troposphere due to high pyroCb activity during the summer wildfire season, which can influence upper tropospheric composition and chemistry (e.g., ozone production). However, significant stratospheric penetration is not observed in the averages.

3.2 Stratospheric smoke signatures

Inspection of every individual occultation measured by ACE-FTS over the 40 to 70°N latitude band in the 2023 burning season revealed a few occultations indicative of stratospheric smoke, exhibited by enhanced chemical signatures and aerosol extinction above the tropopause. These measurements offer evidence of a small amount of smoke in the lowermost stratosphere. The July occultations that exhibit multiple biomass-burning products and aerosol extinction measured in the stratosphere are shown in Fig. 3, and similar profiles for other months are shown in Fig. S5.

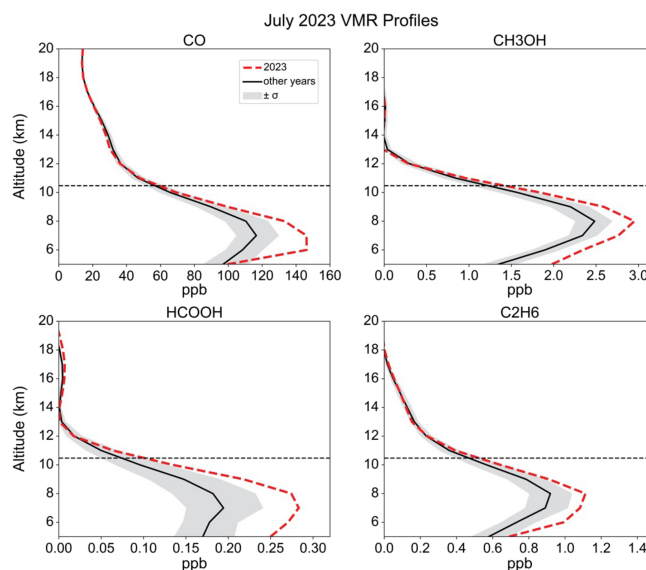


Figure 2. Average July 2023 VMR profiles for additional biomass-burning tracers: CO, CH₃OH, HCOOH, and C₂H₆, plotted against 2004–2022 July averages over 40 to 70°N. The grey-shaded area represents ± 1 standard deviation based on 2004–2022 data.

Elevated VMRs of multiple biomass-burning products measured above the tropopause in these data offer evidence of a nominal amount of wildfire smoke in the stratosphere. To further validate this conclusion, the ACE infrared absorption spectra were also analyzed for features characteristic of wildfire smoke, as in Boone et al. (2020). Carbonaceous aerosols typically exhibit C–H, O–H, and C–C features associated with alkanes and oxygenated organics, and these are indeed present for these occultations, for example as shown in the

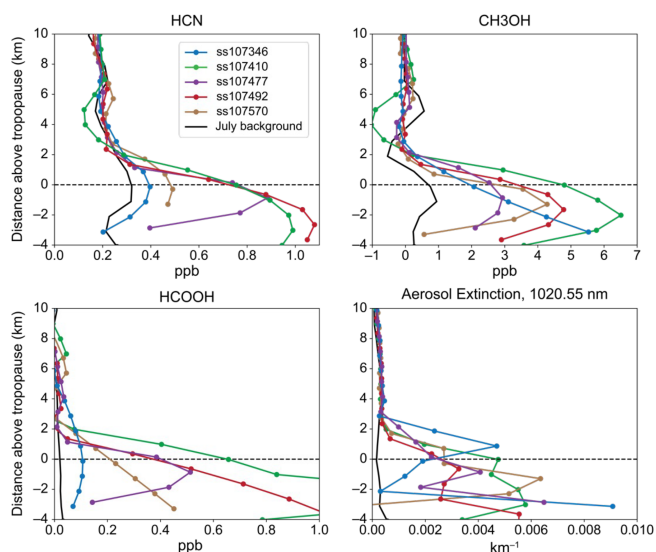


Figure 3. Tropopause-relative profiles for July 2023 occultations that exhibit enhanced wildfire product VMRs and aerosol extinction in the lower stratosphere. A background profile with no smoke from a similar location in July 2023, ss107249, is plotted for reference.

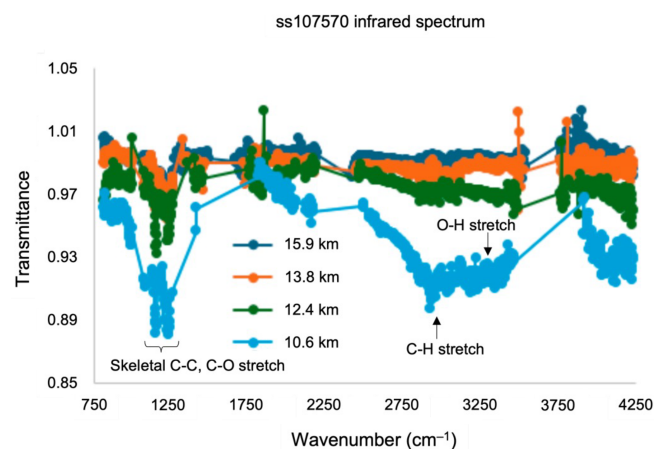


Figure 4. Residual IR spectrum for ss107570 measured at multiple tangent heights. The highlighted features at 10.6 km are indicative of smoke. At higher altitudes, the spectrum becomes plume-free, and there are no longer indicators of smoke.

IR spectrum in Fig. 4 (Zhong and Jang, 2014; Boone et al., 2020; Bernath, 2020). The O–H stretch is commonly seen in smoke particles and indicates that they are oxygenated (Boone et al., 2020). The C=O stretch, which is also associated with oxygenated smoke particles and identified using a feature around 1750 cm^{-1} , cannot be seen because that region is saturated at lower altitudes by strong absorption of water vapor in the same spectral region.

Given the extent of Canada's wildfire season, using fire databases to identify potential source fires is non-trivial given the large number of events in 2023 with extensive

burned areas (Canadian Interagency Forest Fire Centre, 2024, <https://www.cifc.ca/publications/canada-reports>, last access: 17 October 2024). Thus, more targeted methods for identifying pyroCb-specific fires are a more promising approach for this analysis. Cross-referencing with an online crowdsourced pyroCb database (<https://groups.io/g/pyrocb>, last access: 25 August 2024) suggests a few pyroCb events with brightness temperatures below $-55\text{ }^{\circ}\text{C}$. A cold cloud top of this magnitude is indicative of deep overshooting convection that may penetrate the tropopause and enter the stratosphere (Romps and Kuang, 2009). It is therefore plausible that these pyroCbs injected smoke into the stratosphere.

Back trajectories initialized from ACE stratospheric smoke measurements on NOAA HYSPLIT with GDAS 1° meteorological data do not directly intercept any of these reported pyroCbs, but this is not surprising given the limited spatial coverage of ACE (Stein et al., 2015). Trajectories initialized from two occultations, ss107346 and ss107570, pass within tens of kilometers and a few hours of reported pyroCbs (Fig. S6). Despite the lack of direct detection, chemical signatures of smoke after dispersion in the lower stratosphere are clearly measured and show the limited vertical range of wildfire influence in the stratosphere: within 2 km above the tropopause.

3.3 OMPS LP aerosol data

Aerosol extinction data from OMPS LP also indicate a minor increase in aerosol burden in the lower stratosphere averaged between 11.5 and 16.5 km, in late July 2023 (Fig. 5). However, this increase above background levels is both small in magnitude and short-lived, which indicates that not enough smoke was injected into the stratosphere to significantly impact extinction measurements. Throughout the entire wildfire season, there are no significant aerosol extinction signals at this altitude range that would suggest deep convective wildfire events. This validates our general finding that very little smoke managed to make it well above the tropopause despite high pyroCb activity, suggesting that the many convective events that occurred were mostly limited to the upper troposphere. There is a constant background level of aerosols above 60° N , but this feature is present from the beginning of 2023. Therefore, it is not linked to the 2023 Canadian wildfire events but rather to other aerosol sources such as volcanic eruptions.

The altitude range between 10.5 and 11.5 km contains either tropospheric or stratospheric air depending on the latitude and time of year, and an analysis of OMPS data at this altitude reveals substantial average aerosol loading in the region around the tropopause in 2023 (Fig. 8, middle panel). This suggests that the many pyroCbs of the 2023 wildfire season alongside other aerosol sources managed to inject particles right around the tropopause. However, the significantly lower aerosol extinction signal past 11.5 km as seen in Figs. 5 and S7 constrains these inputs to the region at or

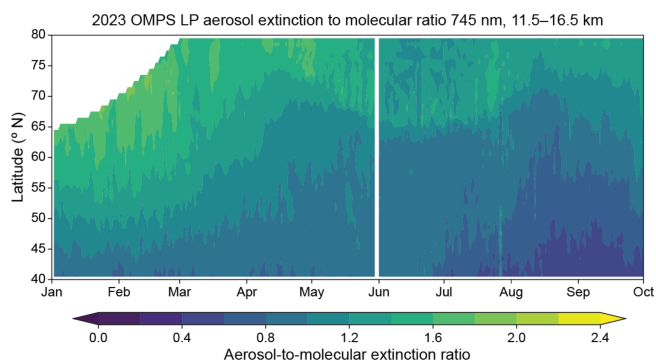


Figure 5. Zonally averaged daily OMPS aerosol-to-molecular extinction ratio between 11.5 and 16.5 km, 40 to 80° N. This represents the evolution of the average aerosol load in the lower stratosphere during the 2023 summer wildfires.

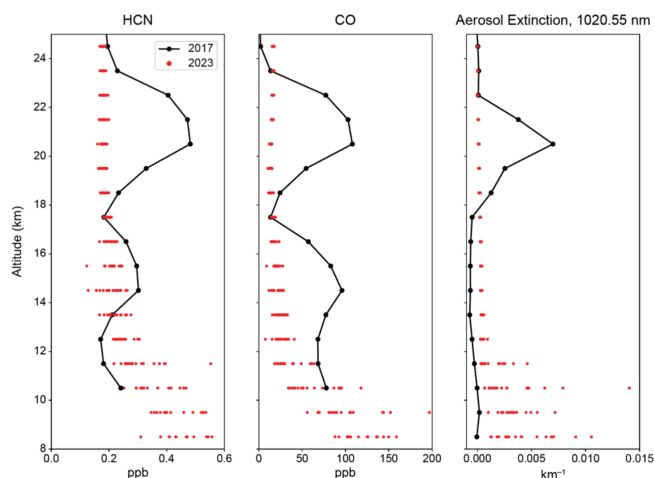


Figure 6. Biomass-burning product VMR and aerosol extinction profiles for occultation sr75758 (black) associated with the 2017 Pacific Northwest Event (Boone et al., 2020). Profiles from the 2023 Canadian wildfires that exhibited stratospheric penetration are shown in red for comparison.

just above the tropopause as opposed to higher in the stratosphere, where more impacts would be realized.

3.4 Comparison to Pacific Northwest Event

To contextualize the 2023 Canadian events, we compare its ACE-FTS profiles with measurements of the 2017 PNE, which also occurred in western Canada during the summer. Analysis of this event was previously reported in Boone et al. (2020), with the occultation sr75758 probing the plume a few weeks after initial stratospheric injection. Figure 6 shows a substantial difference in smoke altitude, with the 2017 PNE leading to chemical signatures of biomass-burning products measured above 20 km compared to the much lower vertical extent of the 2023 fires.

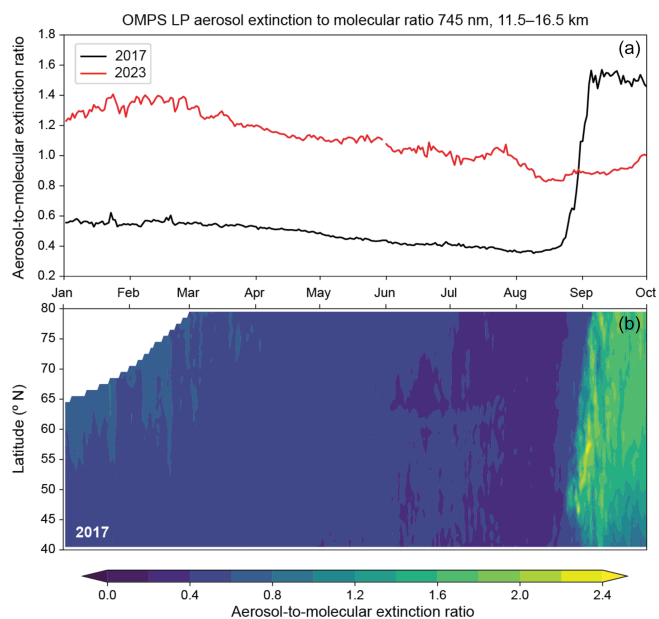


Figure 7. (a) Average OMPS aerosol-to-molecular extinction ratio from 40 and 80° N, 11.5 to 16.5 km, compared between 2017 (black) and 2023 (red). (b) The 2017 zonally averaged OMPS extinction between 11.5 and 16.5 km, 40 to 80° N.

The top panel of Fig. 7 also shows with OMPS data that 2017 featured a much larger injection of aerosols between 11.5 and 16.5 km relative to 2023, where there is no evident increase in average stratospheric aerosol extinction throughout the entire summer. Similarly, the bottom panel of Fig. 7, compared to Fig. 5, shows that the magnitude and duration of stratospheric perturbation from the PNE were much more substantial than those of any pyroCb activity from 2023. Since ACE-FTS measured only a handful of occultations with stratospheric signatures of smoke and the OMPS LP aerosol data do not feature any significant perturbations in 2023 past 12 km, we conclude that the 2023 Canadian wildfire season did not significantly impact stratospheric composition relative to previous years despite burning a far larger area and exhibiting frequent pyroCb activity.

However, the aerosol loading near the tropopause is similar between the 2 years, as seen in Fig. 8. It is clear that the active pyroCb activity in the 2023 wildfire season did influence upper tropospheric composition given the increase in aerosol extinction starting in May, which coincides with the start of the burning season. This is in stark contrast to the stratospheric aerosol loading from Fig. 5, which is the largest at the beginning of the year. Thus, the stratospheric impact of the 2017 PNE is visibly more significant since smoke following the event is measured well above the tropopause, whereas smoke from the 2023 fires remains around the tropopause throughout the entire wildfire season. This lower altitude of perturbation corresponds to a shorter smoke lifetime in the

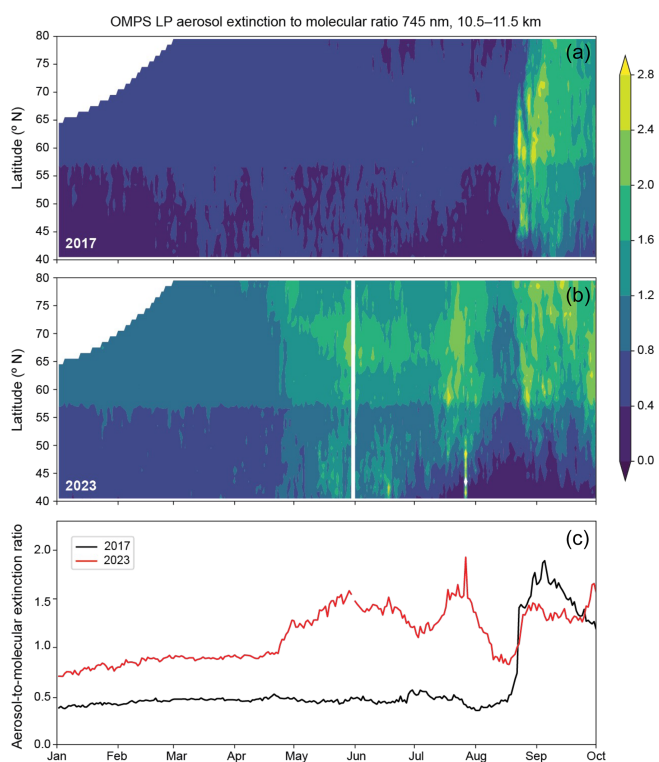


Figure 8. (a) The 2017 zonally averaged OMPS aerosol-to-molecular extinction ratio between 10.5 and 11.5 km, 40 to 80° N. (b) The 2023 zonally averaged OMPS aerosol-to-molecular extinction ratio between 10.5 and 11.5 km, 40 to 80° N. (c) Average OMPS aerosol-to-molecular extinction ratio from 40 to 80° N, 10.5 to 11.5 km, compared between 2017 (black) and 2023 (red).

stratosphere, further suggesting the lower impact of the 2023 fires compared to the PNE (D'Angelo et al., 2022).

4 Conclusions

Using ACE-FTS observations, we identified the presence of biomass-burning products in the stratosphere in a limited number of occultation measurements over Canada during the 2023 summer wildfire season. This and ACE imager data, alongside OMPS LP aerosol data and MLS CO data, suggest that the immediate impacts of these fires are essentially limited to the troposphere, with evidence only for nominal amounts of smoke in the lowermost stratosphere. Any aerosols that made it into the stratosphere remained near the tropopause and did not make it high enough to substantially influence stratospheric composition. However, carbonaceous aerosol has the potential to increase parcel buoyancy via solar heating and to self-loft over longer timescales (de Laat et al., 2012; Yu et al., 2019; Ohneiser et al., 2023). The impacts of this process have not been pursued in this work but may have implications for climate and stratospheric composition. Additionally, the climate implications of increased smoke in

the upper troposphere is an active area of interest (Christian et al., 2019; Kochanski et al., 2019; Li et al., 2021).

In summary, this work shows that despite an extremely extensive wildfire season with frequent pyroCb activity in Canada, the conditions for sufficiently deep convection were met so rarely and to such a limited extent that no significant stratospheric perturbation took place. These results highlight that area alone is not a useful indicator of the potential for stratospheric effects, and projected increases in area burned per degree of global warming are not enough to forecast the vertical extents of future wildfires. The complexity of intense pyroCb formation motivates further study of why certain events, such as the 2019–2020 ANYSO and 2017 PNE, are more primed for stratospheric penetration. Factors including fire intensity and atmospheric structure may play an important role. Understanding which wildfire conditions enable stratospheric impacts, as well as how and where these may be realized under a changing climate, has significant implications for stratospheric ozone and climate.

Code availability. The code used in this study is available upon request from Selena Zhang (selenaxz@mit.edu).

Data availability. The ACE-FTS Level 2 dataset used in this study is available with registration at https://database.scisat.ca/level2/ace_v5.2/ (Boone et al., 2023). First-time users can register at <https://database.scisat.ca/12signup.php> (last access: 25 August 2024). MLS data are available at https://disc.gsfc.nasa.gov/datacollection/ML2CO_NRT_005.html (EOS MLS Science Team, 2022). OMPS LP data are available at <https://doi.org/10.5067/CX2B9NW6FI27> (Taha, 2020). ERA5 hourly data are available at <https://doi.org/10.24381/cds.adbb2d47> (Hersbach et al., 2023).

Supplement. The supplement related to this article is available online at: <https://doi.org/10.5194/acp-24-11727-2024-supplement>.

Author contributions. SS initiated the research. SZ designed the research framework, analyzed the data, and produced the figures. CDB processed the ACE-FTS infrared spectra and contributed to interpretation of the ACE data. GT contributed to OMPS LP data interpretation. SZ wrote the paper.

Competing interests. The contact author has declared that none of the authors has any competing interests.

Disclaimer. Publisher's note: Copernicus Publications remains neutral with regard to jurisdictional claims made in the text, published maps, institutional affiliations, or any other geographical representation in this paper. While Copernicus Publications makes ev-

ery effort to include appropriate place names, the final responsibility lies with the authors.

Acknowledgements. Selena Zhang was funded by an MIT John H. Olsen Presidential Fellowship. Funding for the Atmospheric Chemistry Experiment was provided by the Canadian Space Agency.

Financial support. This research has been supported by the National Science Foundation Division of Atmospheric and Geospace Sciences (grant no. 2316980), an MIT John H. Olsen Presidential Fellowship, and the Canadian Space Agency.

Review statement. This paper was edited by Matthias Tesche and reviewed by Michael Fromm and three anonymous referees.

References

- Basha, G., Ratnam, M. V., and Kishore, P.: Asian summer monsoon anticyclone: trends and variability, *Atmos. Chem. Phys.*, 20, 6789–6801, <https://doi.org/10.5194/acp-20-6789-2020>, 2020.
- Bernath, P. F.: Atmospheric Chemistry Experiment (ACE): Mission Overview, Fourier Transform Spectroscopy/ Hyperspectral Imaging and Sounding of the Environment, Optica Publishing Group, <https://doi.org/10.1364/FTS.2005.JMA3>, 2005.
- Bernath, P. F.: The Atmospheric Chemistry Experiment (ACE), *J. Quant. Spectrosc. Ra.*, 186, 3–16, <https://doi.org/10.1016/j.jqsrt.2016.04.006>, 2017.
- Bernath, P.: Vibrational Spectroscopy, in: *Spectra of Atoms and Molecules*, 4th edn., Oxford University Press, Oxford, p. 260, ISBN 0190095407, 2020.
- Bernath, P., Boone, C., and Crouse, J.: Wildfire Smoke Destroys Stratospheric Ozone, *Science*, 375, 1292–1295, <https://doi.org/10.1126/science.abm5611>, 2022.
- Boone, C. D., Bernath, P. F., and Fromm, M. D.: Pyrocumulonimbus Stratospheric Plume Injections Measured by the ACE-FTS, *Geophys. Res. Lett.*, 47, e2020GL088442, <https://doi.org/10.1029/2020GL088442>, 2020.
- Boone, C. D., Bernath, P. F., and Lecours, M.: Version 5 Retrievals for ACE-FTS and ACE-Imagers, *J. Quant. Spectrosc. Ra.*, 310, 108749, <https://doi.org/10.1016/j.jqsrt.2023.108749>, 2023 (data available at: https://database.scisat.ca/level2/ace_v5.2/, last access: 25 August 2024).
- Boer, M. M., de Dios, R., and Bradstock, R. A.: Unprecedented burn area of Australian mega forest fires, *Nat. Clim. Change*, 10, 170–172, <https://doi.org/10.1038/s41558-020-0716-1>, 2020.
- Buijs, H. L., Soucy, M.-A., and Lachance, R. L.: ACE-FTS Hardware and Level 1 Processing, in: *The Atmospheric Chemistry Experiment ACE at 10: A Solar Occultation Anthology*, edited by: Bernath, P. F., A. Deepak Publishing, Virginia, 53–80, ISBN 0937194549, 2013.
- Canadian Interagency Forest Fire Centre: Canada Report 2023 Fire Season, <https://www.ciffc.ca/publications/canada-reports>, last access: 17 October 2024.
- Canadian Interagency Forest Fire Centre Inc.: Wildfire Graphs, <https://ciffc.net/statistics/>, last access: 10 January 2024.
- Chen, Z., DeLand, M., and Bhartia, P. K.: A new algorithm for detecting cloud height using OMPS/LP measurements, *Atmos. Meas. Tech.*, 9, 1239–1246, <https://doi.org/10.5194/amt-9-1239-2016>, 2016.
- Christian, K., Wang, J., Ge, C., Peterson, D., Hyer, E., Yorks, J., and McGill, M.: Radiative Forcing and Stratospheric Warming of Pyrocumulonimbus Smoke Aerosols: First Modeling Results With Multisensor (EPIC, CALIPSO, and CATS) Views from Space, *Geophys. Res. Lett.*, 46, 10061–10071, <https://doi.org/10.1029/2019GL082360>, 2019.
- D’Angelo, G., Guimond, S., Reisner, J., Peterson, D. A., and Dubey, M.: Contrasting Stratospheric Smoke Mass and Lifetime From 2017 Canadian and 2019/2020 Australian Megafires: Global Simulations and Satellite Observations, *J. Geophys. Res.-Atmos.*, 127, e2021JD036249, <https://doi.org/10.1029/2021JD036249>, 2022.
- Davey, S. M. and Sarre, A.: Editorial: the 2019/20 Black Summer bushfires, *Aust. For.*, 83, 47–51, <https://doi.org/10.1080/00049158.2020.1769899>, 2020.
- De Laat, A. T. J., Stein Zweers, D. C., Boers, R., and Tuinder, O. N. E.: A solar escalator: Observational evidence of the self-lifting of smoke and aerosols by absorption of solar radiation in the February 2009 Australian Black Saturday plume, *J. Geophys. Res.-Atmos.*, 117, D04204, <https://doi.org/10.1029/2011JD017016>, 2012.
- Di Virgilio, G., Evans, J. P., Blake, S. A., Armstrong, M., Dowdy, A. J., Sharples, J., and McRae, R.: Climate Change Increases the Potential for Extreme Wildfires, *Geophys. Res. Lett.*, 46, 8517–8526, <https://doi.org/10.1029/2019GL083699>, 2019.
- Doeringer, D., Eldering, A., Boone, C. D., González Abad, G., and Bernath, P. F.: Observation of sulfate aerosols and SO₂ from the Sarychev volcanic eruption using data from the Atmospheric Chemistry Experiment (ACE), *J. Geophys. Res.-Atmos.*, 117, D03203, <https://doi.org/10.1029/2011JD016556>, 2012.
- EOS MLS Science Team: MLS/Aura Near-Real-Time L2 Carbon Monoxide (CO) Mixing Ratio V005, Greenbelt, MD, USA, Goddard Earth Sciences Data and Information Services Center (GES DISC) [data set], https://disc.gsfc.nasa.gov/datacollection/ML2CO_NRT_005.html (last access: 25 August 2024), 2022.
- Fromm, M., Lindsey, D. T., Servranckx, R., Yue, G., Trickl, T., Sica, R., Doucet, P., and Godin-Beekmann, S.: The Untold Story of Pyrocumulonimbus, *B. Am. Meteorol. Soc.*, 91, 1193–1210, <https://doi.org/10.1175/2010BAMS3004.1>, 2010.
- Fromm, M., Peterson, D., and Di Girolamo, L.: The Primary Convective Pathway for Observed Wildfire Emissions in the Upper Troposphere and Lower Stratosphere: A Targeted Reinterpretation, *J. Geophys. Res.*, 124, 13254–13272, <https://doi.org/10.1029/2019JD031006>, 2019.
- Fromm, M., Servranckx, R., Stocks, B. J., and Peterson, D. A.: Understanding the Critical Elements of the Pyrocumulonimbus Storm Sparked by High-Intensity Wildland Fire, *Commun. Earth Environ.*, 3, 243, <https://doi.org/10.1038/s43247-022-00566-8>, 2022.
- Government of British Columbia: <https://www2.gov.bc.ca/gov/content/safety/wildfire-status/about-bcws/wildfire-history/wildfire-season-summary>, last access: 10 January 2024.

- Hersbach, H., Bell, B., Berrisford, P., Biavati, G., Horányi, A., Muñoz Sabater, J., Nicolas, J., Peubey, C., Radu, R., Rozum, I., Schepers, D., Simmons, A., Soci, C., Dee, D., and Thépaut, J.-N.: ERA5 hourly data on single levels from 1940 to present, Copernicus Climate Change Service (C3S) Climate Data Store (CDS) [data set], <https://doi.org/10.24381/cds.adbb2d47>, 2023.
- Homeyer, C. R., Pan, L. L., Dorsi, S. W., Avallone, L. M., Weinheimer, A. J., O'Brien, A. S., DiGangi, J. P., Zondlo, M. A., Ryerson, T. B., Diskin, G. S., and Campos, T. L.: Convective transport of water vapor into the lower stratosphere observed during double-tropopause events, *J. Geophys. Res.-Atmos.*, 119, 10941–10958, <https://doi.org/10.1002/2014JD021485>, 2014.
- Kablick III, G. P., Allen, D. R., Fromm, M. D., and Nedoluha, G. E.: Australian PyroCb Smoke Generates Synoptic-Scale Stratospheric Anticyclones, *Geophys. Res. Lett.*, 47, e2020GL088101, <https://doi.org/10.1029/2020GL088101>, 2020.
- Khaykin, S., Legras, B., Bucci, S., Sellitto, P., Isaksen, I., Tencé, F., Bekki, S., Bourassa, A., Rieger, L., Zawada, D., Jumelet, J., and Godin-Beekmann, S.: The 2019/20 Australian wildfires generated a persistent smoke-charged vortex rising up to 35km altitude, *Commun. Earth Environ.*, 1, 22, <https://doi.org/10.1038/s43247-020-00022-5>, 2020.
- Kochanski, A. K., Mallia, D. V., Fearon, M. G., Mandel, J., Souri, A. H., and Brown, T.: Modeling Wildfire Smoke Feedback Mechanisms Using a Coupled Fire-Atmosphere Model With a Radiatively Active Aerosol Scheme, *J. Geophys. Res.-Atmos.*, 124, 9099–9116, <https://doi.org/10.1029/2019JD030558>, 2019.
- Lestrelin, H., Legras, B., Podglajen, A., and Salihoglu, M.: Smoke-charged vortices in the stratosphere generated by wildfires and their behaviour in both hemispheres: comparing Australia 2020 to Canada 2017, *Atmos. Chem. Phys.*, 21, 7113–7134, <https://doi.org/10.5194/acp-21-7113-2021>, 2021.
- Li, Q., Jacob, D. J., Bey, I., Yantosca, R. M., Zhao, Y., Kondo, Y., and Notholt, J.: Atmospheric Hydrogen Cyanide (HCN): Biomass Burning Source, Ocean Sink?, *Geophys. Res. Lett.*, 27, 357–360, <https://doi.org/10.1029/1999gl1010935>, 2000.
- Li, Y., Dykema, J., Deshler, T., and Keutsch, F.: Composition Dependence of Stratospheric Aerosol Shortwave Radiative Forcing in Northern Midlatitudes, *Geophys. Res. Lett.*, 48, e2021GL094427, <https://doi.org/10.1029/2021GL094427>, 2021.
- Livesey, N. J., Read, W. G., Wagner, P. A., Froidevaux, L., Santee, M. L., Schwartz, M. J., Lambert, A., Valle, L. F. M., Pumphrey, H. C., Manney, G. L., Fuller, R. A., Jarnot, R. F., Knosp, B. W., and Lay, R. R.: Version 5.0x Level 2 and 3 data quality and description document, Tech. Rep. JPL D-105336 Rev. B, Jet Propulsion Laboratory, California Institute of Technology, Pasadena, California, https://mls.jpl.nasa.gov/data/v5-0_data_quality_document.pdf (last access: 21 January 2024), 2022.
- Loughman, R., Bhartia, P. K., Chen, Z., Xu, P., Nyaku, E., and Taha, G.: The Ozone Mapping and Profiler Suite (OMPS) Limb Profiler (LP) Version 1 aerosol extinction retrieval algorithm: theoretical basis, *Atmos. Meas. Tech.*, 11, 2633–2651, <https://doi.org/10.5194/amt-11-2633-2018>, 2018.
- MODIS Land Rapid Response Team: July 5, 2023 – Fire and Smoke in Russia's Far East, NASA GSFC, https://modis.gsfc.nasa.gov/gallery/individual.php?db_date=2023-07-05 (last access: 27 February 2024), 2023.
- Ohneiser, K., Ansmann, A., Witthuhn, J., Deneke, H., Chudnovsky, A., Walter, G., and Senf, F.: Self-lofting of wildfire smoke in the troposphere and stratosphere: simulations and space lidar observations, *Atmos. Chem. Phys.*, 23, 2901–2925, <https://doi.org/10.5194/acp-23-2901-2023>, 2023.
- Pausas, J. G. and Keeley, J. E.: Wildfires and Global Change, *Front. Ecol. Environ.*, 19, 387–395, <https://doi.org/10.1002/fee.2359>, 2021.
- Peevey, T. R., Gille, J. C., Randall, C. E., and Kunz, A.: Investigation of double tropopause spatial and temporal global variability utilizing High Resolution Dynamics Limb Sounder temperature observations, *J. Geophys. Res.-Atmos.*, 117, D01105, <https://doi.org/10.1029/2011JD016443>, 2012.
- Peterson, D. A., Hyer, E. J., Campbell, J. R., Solbrig, J. E., and Fromm, M. D.: A Conceptual Model for Development of Intense Pyrocumulonimbus in Western North America, *Mon. Weather Rev.*, 145, 2235–2255, <https://doi.org/10.1175/MWR-D-16-0232.1>, 2017.
- Peterson, D. A., Campbell, J. R., Hyer, E. J., Fromm, M. D., Kablick III, G. P., Cossuth, J. H., and Deland, M. T.: Wildfire-driven thunderstorms cause a volcano-like stratospheric injection of smoke, *npj Clim. Atmos. Sci.*, 1, 30, <https://doi.org/10.1038/s41612-018-0039-3>, 2018.
- Peterson, D. A., Fromm, M. D., McRae, R. H. D., Campbell, J. R., Hyer, E. J., Taha, G., Camacho, C. P., Kablick III, G. P., Schmidt, C. C., and DeLand, M. T.: Australia's Black Summer pyrocumulonimbus super outbreak reveals potential for increasingly extreme stratospheric smoke events, *npj Clim. Atmos. Sci.*, 4, 38, <https://doi.org/10.1038/s41612-021-00192-9>, 2021.
- Renard, J.-B., Berthet, G., Levasseur-Regourd, A.-C., Beresnev, S., Miffre, A., Rairoux, P., Vignelles, D., and Jégou, F.: Origins and Spatial Distribution of Non-Pure Sulfate Particles (NSPs) in the Stratosphere Detected by the Balloon-Borne Light Optical Aerosols Counter (LOAC), *Atmosphere*, 11, 1031, <https://doi.org/10.3390/atmos11101031>, 2020.
- Rieger, L. A., Randel, W. J., Bourassa, A. E., and Solomon, S.: Stratospheric Temperature and Ozone Anomalies Associated With the 2020 Australian New Year Fires, *Geophys. Res. Lett.*, 48, e2021GL095898, <https://doi.org/10.1029/2021GL095898>, 2021.
- Roberts, J. M., Stockwell, C. E., Yokelson, R. J., de Gouw, J., Liu, Y., Selimovic, V., Koss, A. R., Sekimoto, K., Coggon, M. M., Yuan, B., Zarzana, K. J., Brown, S. S., Santin, C., Doerr, S. H., and Warneke, C.: The nitrogen budget of laboratory-simulated western US wildfires during the FIREX 2016 Fire Lab study, *Atmos. Chem. Phys.*, 20, 8807–8826, <https://doi.org/10.5194/acp-20-8807-2020>, 2020.
- Romps, D. M. and Kuang, Z.: Overshooting convection in tropical cyclones, *Geophys. Res. Lett.*, 36, L09804, <https://doi.org/10.1029/2009GL037396>, 2009.
- Sellitto, P., Belhadji, R., Cuesta, J., Podglajen, A., and Legras, B.: Radiative impacts of the Australian bushfires 2019–2020 – Part 2: Large-scale and in-vortex radiative heating, *Atmos. Chem. Phys.*, 23, 15523–15535, <https://doi.org/10.5194/acp-23-15523-2023>, 2023.
- Sica, R. J., Izawa, M. R. M., Walker, K. A., Boone, C., Petelina, S. V., Argall, P. S., Bernath, P., Burns, G. B., Catoire, V., Collins, R. L., Daffer, W. H., De Clercq, C., Fan, Z. Y., Firanski, B. J., French, W. J. R., Gerard, P., Gerding, M., Granville, J., Innis, J. L., Keckhut, P., Kerzenmacher, T., Klekociuk, A. R., Kyrö, E., Lambert, J. C., Llewellyn, E. J., Manney, G. L., McDer-

- mid, I. S., Mizutani, K., Murayama, Y., Piccolo, C., Raspollini, P., Ridolfi, M., Robert, C., Steinbrecht, W., Strawbridge, K. B., Strong, K., Stübi, R., and Thuraijajah, B.: Validation of the Atmospheric Chemistry Experiment (ACE) version 2.2 temperature using ground-based and space-borne measurements, *Atmos. Chem. Phys.*, 8, 35–62, <https://doi.org/10.5194/acp-8-35-2008>, 2008.
- Smith, J. M.: Data Chat: Dr. David Peterson, <https://www.earthdata.nasa.gov/learn/data-chats/david-peterson> (last access: 3 February 2024), 2023.
- Solomon, S., Stone, K., Yu, P., Murphy, D. M., Kinnison, D., Ravishankara, A. R., and Wang, P.: Chlorine activation and enhanced ozone depletion induced by wildfire aerosol, *Nature*, 615, 259–264, <https://doi.org/10.1038/s41586-022-05683-0>, 2023.
- Stein, A. F., Draxler, R. R., Rolph, G. D., Stunder, B. J. B., Cohen, M. D., and Ngan, F.: NOAA's HYSPLIT Atmospheric Transport and Dispersion Modeling System, *B. Am. Meteorol. Soc.*, 96, 2059–2077, <https://doi.org/10.1175/BAMS-D-14-00110.1>, 2015.
- Taha, G.: OMPS-NPP L2 LP Aerosol Extinction Vertical Profile swath daily 3slit V2, Greenbelt, MD, USA, Goddard Earth Sciences Data and Information Services Center (GES DISC) [data set], <https://doi.org/10.5067/CX2B9NW6FI27>, 2020.
- Taha, G., Loughman, R., Zhu, T., Thomason, L., Kar, J., Rieger, L., and Bourassa, A.: OMPS LP Version 2.0 multi-wavelength aerosol extinction coefficient retrieval algorithm, *Atmos. Meas. Tech.*, 14, 1015–1036, <https://doi.org/10.5194/amt-14-1015-2021>, 2021.
- Taha, G., Loughman, R., Colarco, P. R., Zhu, T., Thomason, L. W., and Jaross, G.: Tracking the 2022 Hunga Tonga-Hunga Ha'apai Aerosol Cloud in the Upper and Middle Stratosphere Using Space-Based Observations, *Geophys. Res. Lett.*, 49, e2022GL100091, <https://doi.org/10.1029/2022GL100091>, 2022.
- Thurston, G., Yu, W., and Luglio, D.: An Evaluation of the Asthma Impact of the June 2023 New York City Wildfire Air Pollution Episode, *Am. J. Resp. Crit. Care*, 208, 898–900, <https://doi.org/10.1164/rccm.202306-1073LE>, 2023.
- Torres, O., Bhartia, P. K., Taha, G., Jethva, H., Das, S., Colarco, P., Krotkov, N., Omar, A., and Ahn, C.: Stratospheric Injection of Massive Smoke Plume From Canadian Boreal Fires in 2017 as Seen by DSCOVR-EPIC, CALIOP, and OMPS-LP Observations, *J. Geophys. Res.-Atmos.*, 125, e2020JD032579, <https://doi.org/10.1029/2020JD032579>, 2020.
- Vanhellemont, F., Tetard, C., Bourassa, A., Fromm, M., Dodion, J., Fussen, D., Brogniez, C., Degenstein, D., Gilbert, K. L., Turnbull, D. N., Bernath, P., Boone, C., and Walker, K. A.: Aerosol extinction profiles at 525 nm and 1020 nm derived from ACE imager data: comparisons with GOMOS, SAGE II, SAGE III, POAM III, and OSIRIS, *Atmos. Chem. Phys.*, 8, 2027–2037, <https://doi.org/10.5194/acp-8-2027-2008>, 2008.
- Wang, Z., Wang, Z., Zou, Z., Chen, X., Wu, H., Wang, W., Su, H., Li, F., Xu, W., Liu, Z., and Zhu, J.: Severe Global Environmental Issues Caused by Canada's Record-Breaking Wildfires in 2023, *Adv. Atmos. Sci.*, 41, 565–571, <https://doi.org/10.1007/s00376-023-3241-0>, 2023.
- Waters, J., Froidevaux, L., Harwood, R., Jarnot, R., Pickett, H., Read, W., Siegel, P., Cofield, R., Filipiak, M., Flower, D., Holden, J., Lau, G., Livesey, N., Manney, G., Pumphrey, H., Santee, M., Wu, D., Cuddy, D., Lay, R., Loo, M., Perun, V., Schwartz, M., Stek, P., Thurstans, R., Boyles, M., Chandra, K., Chavez, M., Chen, G.-S., Chudasama, B., Dodge, R., Fuller, R., Girard, M., Jiang, J., Jiang, Y., Knosp, B., LaBelle, R., Lam, J., Lee, K., Miller, D., Oswald, J., Patel, N., Pukala, D., Quintero, O., Scaff, D., Van Snyder, W., Tope, M., Wagner, P., and Walch, M.: The earth observing system microwave limb sounder (EOS MLS) on the Aura satellite, *IEEE T. Geosci. Remote*, 44, 1075–1092, <https://doi.org/10.1109/TGRS.2006.873771>, 2006.
- Williams, A. P., Abatzoglou, J. T., Gershunov, A., Guzman-Morales, J., Bishop, D. A., Balch, J. K., and Lettenmaier, D. P.: Observed Impacts of Anthropogenic Climate Change on Wildfire in California, *Earths Future*, 7, 892–910, <https://doi.org/10.1029/2019EF001210>, 2019.
- World Meteorological Organization (WMO): Meteorology – A three-dimensional science: Second session of the commission for aerology, *WMO Bull.*, 4, 134–138, 1957.
- Xiao, Y., Jacob, D. J., Wang, J. S., Logan, J. A., Palmer, P. I., Suntharalingam, P., Yantosca, R. M., Sachse, G. W., Blake, D. R., and Streets, D. G.: Constraints on Asian and European sources of methane from CH₄-C₂H₆-CO correlations in Asian outflow, *J. Geophys. Res.-Atmos.*, 109, D15S16, <https://doi.org/10.1029/2003JD004475>, 2004.
- Yu, P., Toon, O. B., Bardeen, C. G., Zhu, Y., Rosenlof, K. H., Portmann, R. W., Thornberry, T. D., Gao, R.-S., Davis, S. M., Wolf, E. T., de Gouw, J., Peterson, D. A., Fromm, M. D., and Robock, A.: Black carbon lofted wildfire smoke high into the stratosphere to form a persistent plume, *Science*, 365, 587–590, <https://doi.org/10.1126/science.aax1748>, 2019.
- Zhong, M. and Jang, M.: Dynamic light absorption of biomass-burning organic carbon photochemically aged under natural sunlight, *Atmos. Chem. Phys.*, 14, 1517–1525, <https://doi.org/10.5194/acp-14-1517-2014>, 2014.